DOI: 10.13009/EUCASS2023-396
Aerospace Europe Conference 2023 – 10TH EUCASS – 9TH CEAS

Multi-phase Robust Optimization of a Hybrid Guidance Architecture for Launch Vehicles

Akan Selim⋆† *and İbrahim Özkol*∗
⋆*Istanbul Technical University, Maslak, Istanbul, Türkiye*
∗*Istanbul Technical University, Aviation Institute, Maslak, Istanbul, Türkiye*
selim16@itu.edu.tr · ozkol@itu.edu.tr
†Corresponding author

Abstract

A novel computational framework is developed to optimize both robust open-loop and closed-loop guidance modes under uncertainties. Multi-phase launch vehicle optimization problems, including achieving insertion into a Geostationary-Transfer Orbit (GTO) and executing a Return to Launch Site (RTLS) maneuver under constraints is studied. The framework effectively considers uncertainties in thrust, aerodynamic coefficients, atmospheric density, and specific impulse by employing Stochastic-Collocation based Ensemble Pseudospectral Optimal Control Software (SC-EPOCS), Recovery Ensemble Control (REC), and Conjugate Unscented Transformation (CUT). This approach generates safe and optimal trajectories and trajectory reshaping strategies, thereby mitigating risks and minimizing state dispersions at the end of the open-loop guidance phase.

1. Introduction

Trajectory optimization plays a pivotal role in the design of launch vehicles as it directly impacts the economic feasibility and safety assurance of missions. Epistemic and aleatoric uncertainty quantification and propagation represent a critical technology to increase the robustness against design constraints, minimize the risk of mission failure under uncertainties and systematic way of assigning optimal design margins.

In recent years, the field of space mission design has witnessed a surge of interest in advanced optimization techniques such as convex optimization, indirect optimal control, and pseudospectral methods. However, traditional methods are often limited in their ability to handle the uncertainties and disturbances that are inherent in space missions, leading to suboptimal or even failed missions. In astronautics, uncertainties arise due to several factors such as atmospheric conditions, aerodynamics, propulsion, navigation and system failures. Failure to account for these uncertainties can lead to mission failure or increased costs due to the need for contingency plans. Additional propellant is reserved exclusively for correction maneuvers aimed at compensating for trajectory deviations arising from uncertainties and disturbances. This approach often leads to strategies that are excessively over-conservative, in order to ensure robustness to deviations in trajectory. Robust trajectory optimization techniques help ensure mission success by enabling spacecraft to adapt to unforeseen circumstances, including those that are difficult to predict. By utilizing sophisticated trajectory optimization techniques, trajectories can achieve mission objectives under a wide range of conditions and improve mission success rates, reduce costs, and enable missions that would otherwise be too risky or expensive.

Therefore, there exists a pressing need for a systematic methodology for designing a nominal and robust trajectory, and an associated closed-loop control law that incorporates the information on uncertainties. Optimally reshaping the reference guidance to steer the initial distribution towards a goal is referred to as covariance steering,[1,2] approach in stochastic optimal control. Recently a covariance-control based optimization framework for robust trajectory optimization including navigational errors was introduced with the use of multiple-shooting approach.[3] To make the resulting optimization problem computationally tractable, sequential convex programming was deployed to study stochastic trajectories for solar sail[4] and low-thrust[5] missions under Gaussian uncertainties. A similar approach together with convex optimization was applied to covariance steering of launch vehicles[6] under Gaussian uncertainties by generating optimal robust guidance law based on linear feedback for non-throttleable upper stages.

In pursuit of optimal maneuvers under stochastic disturbances and uncertainties, research has delved into launching into parking orbits, Lambert rendezvous orbits, and Halo-transfer orbits.[7] To tackle with stochastic optimal control problems, Sums-of-Squares[8] and tube-based approaches[9] have been developed to design robust optimal feedback controllers, which transforms the problem into a deterministic optimal control problem, through the utilization of sampling-based approaches such as the Unscented Transformation. The constraints can be incorporated as chance constraints,

DOI: 10.13009/EUCASS2023-396

assuming the uncertainties to be Gaussian processes. The success of academic research on tube-MPC and other tube-based approaches like funnel libraries, SOS, and convex optimization has led to the development of tube stochastic Differential Dynamic Programming[10] and applied to a stochastic low-thrust trajectory optimization. In contrary to these approaches where navigational models are not included into the optimization framework,[11] studied rendezvous in NRHO environment via Linear Covariance Analysis including navigational models under Gaussian assumption and[12] developed an observability aware trajectory design architecture to optimally study the gravitational field of an asteroid. In lieu of designing a robust controller for the solution of stochastic optimal control problems, a robust guidance technique was investigated in[13] for the safe generation of a reference orbit for asteroid approach and landing problem,[14].[15] The methodology is based on convex programming and the chance-constrained formulation. Another approach that relies solely on open-loop control laws is belief optimal control.[16] This formulation results in a transformation of cost and constraint functions into probability distributions, wherein uncertainty propagation is established by modeling both aleatoric and epistemic uncertainties via non-intrusive Polynomial Chaos Expansion. The resulting problem is then solved using multiple-shooting and nonlinear programming.

In the current literature of robust trajectory optimization, these goals are pursued at the expense of employing nested optimization loops with heuristic algorithms or reformulating trajectory optimization as a robust optimal control problem where states and uncertain variables are rewritten in terms of polynomial expansions via non-intrusive Polynomial Chaos Expansion methods.[17] In alternative approaches, their outputs can be used to form a meta-model[18] for Uncertainty Quantification in uncertainty-based Multidisciplinary Optimization studies.[19–21] However, the former approach[22,23] suffers from significant drawbacks, including excessive computational time and no guarantee of local optima. The latter approach relies on nonlinear programming with high-dimensional state spaces[24–27] making convergence challenging, if not impossible, for low-dimensional uncertainties. In response to that, recent methods have been proposed based on convex optimization[28] which requires either a re-formulation of the original constraints as convex constraints or successively linearizing both the dynamics and the constraints. However, this can lead to a compromised optimality of solutions for extended flight durations.

Moreover, most of the aforementioned methodologies that are applied to launch vehicles generate open-loop trajectories with a fixed flight duration for each phase of the flight vehicle including orbital insertion. This conservative approach does not align with the fact that most launch vehicles employ closed-loop guidance algorithms, such as Iterative Guidance Method (IGM),[29] Powered Explicit Guidance (PEG),[29,30] real-time implementable convex solvers[31] like Sequential Pseudospectral Convex Programming (SPCP),[32] xPIPG,[33] Sequential Conic Optimization (SeCO)[34] and DESCENDO.[35]

In order to incorporate the closed-loop guidance phase within trajectory design for exo-atmospheric flight and mitigate the adverse effects of dispersed states at the end of the open-loop guidance phase, a novel computational framework has been devised. This framework enables the optimization of both guidance modes, culminating in a hybrid guidance architecture.

Two benchmark multi-phase launch vehicle optimization problems[36,37] are rewritten as a robust uncertainty-aware trajectory optimization problem with the proposed approach, consisting of open and closed-loop phases in a single nonlinear programming algorithm to maximize the expected payload mass. The approach involves generating a robust open-loop reference trajectory for the endo-atmospheric phase, while independently optimizing the closed-loop guidance phase for each ensemble trajectory. As a generalization of the aforementioned studies in which a robust and an optimal reference trajectory is optimized with a linear feedback term, we utilize the recently developed recovery ensemble control concept for obtaining fractionally robust trajectories and accompanied feedback controls. These feedback control terms can be used to derive these feedback linear matrix gains as the resulting terms are functions of dispersed states, and also, the mean of these trajectories. A recently developed closed-loop robust guidance and control architecture based on Recovery Ensemble Control (REC)[38] is included for that purpose. REC enables the steering of ensembles towards designated endpoints, rather than just an area.

To address uncertainties pertaining to thrust, specific impulse, atmospheric density and aerodynamic coefficients, recently developed Stochastic-Collocation based Ensemble Pseudospectral Optimal Control Software (SC-EPOCS)[39] is employed. This software is an extension of a previously developed optimal control software which was validated for many benchmark deterministic aerospace missions[38] and was used to demonstrate the optimality and feasibility of robust trajectories for high-dimensional uncertainty spaces in a 6-DOF[40] state constrained close-proximity docking maneuver and re-entry.[41]

Sampling from uncertainty space is done in accordance with a quadrature rule generated using the Conjugate Unscented Transformation (CUT),[42] and the robust trajectory optimization problem is reformulated in a vectorized format. This reformulation significantly reduces computational time requirements and ensures robust convergence by appropriately scaling control variables and the objective function based on the number of ensembles. Notably, this approach requires fewer cubature nodes while preserving the nonlinearity of the dynamics in propagating uncertainties. To solve the resulting ensemble trajectories, a mesh generated using the Legendre-Gauss-Radau (LGR) collocation method in the

DOI: 10.13009/EUCASS2023-396

time domain is implemented, alongside the open-source interior-point solver IPOPT.
The proposed architecture offers several notable advantages. Firstly, it enables fast optimization of the guidance architecture while ensuring robustness and optimality. This contributes to increased flight safety by minimizing risks associated with various uncertainties and reduce the state dispersions at the end of the open-loop guidance phase. Consequently, by incorporating the closed-loop phase, the expected value of the deliverable payload is increased and mission constraints are satisfied.
The paper is structured in the following manner: Section 2 the ensemble optimal control problem and sparse-grid based transcription of the robust trajectory optimization is described. Then, Section 3 introduces the two benchmark problems with three case studies. Finally, Section 4 provides a comprehensive comparison of the performance of different guidance architectures.

2. Robust Guidance Optimization

2.1 Ensemble Optimal Control

Ensemble Optimal Control REFEns1 attempts to optimize a single control signal for an ensemble with same dynamics and constraints but different system parameters with uncertainties and initial conditions. The cost functional can be written as,

$$\mathcal{J}(u) := \int_{\Theta} \int_{0}^{1} a(t, x_u^{\theta}, \theta) d\upsilon(t) d\mu(\theta) + \frac{\beta}{2} |u|_{L^2}^2 \tag{1}$$

where, υ, μ are Borel probability measures.
To make the resulting problem numerically solvable, resulting optimal control problem can be approximated via utilizing a finite set of sub-ensembles to replace μ via (μ_N) generated by quadrature rules. Then the functional of the functional is written as,

$$\mathcal{J}^N(u) := \int_{\Theta} \int_{0}^{1} a(t, x_u^{\theta}, \theta) d\upsilon(t) d\mu_N(\theta) + \frac{\beta}{2} |u|_{L^2}^2 \tag{2}$$

To satisfy required high-order statistical moments, quadrature points must be chosen such that the Moment Constraint Equations (MCE) holds. To transform the high-dimensional integration problem into a finite sum, an approximation is made as follows:

$$\mathbb{E}[f(x)] = \int \int \dots \int f(x) p(x) dx_1 dx_2 \dots dx_n \approx \sum_{i=1}^{N} w_i f(x_i) \tag{3}$$

With respect to the quadrature rules, the mean $\hat{x}_t$ and moments M_t of the state variables $x_t^{(i)}$ can be written as,

$$\hat{x}_t \approx \sum_{i=1}^{N} \alpha^{(i)} x_t^{(i)} M_t \approx \sum_{i=1}^{N} \alpha^{(i)} x_t^{(i)} (x_t^{(i)})^T \left\{ x_0^{(i)}, \alpha^{(i)} \right\},\ i = 1, \dots, N \tag{4}$$

Note that the quadrature weights $\alpha^{(i)}$ are constants in time.
A Bolza type optimal control problem (OCP) is then written in terms of ensembles as:

$$\mathcal{J} = \sum_{\theta=1}^{n_{ens}} \alpha_{\theta} \phi_{\theta} \left(e_{\theta}^{(1)}, \dots, e_{\theta}^{(P)} \right) + \sum_{\theta=1}^{n_{ens}} \alpha_{\theta} \sum_{p=1}^{P} \int_{t_0^{(p)}}^{t_f^{(p)}} g_{\theta}^{(p)}(y_{\theta}^{(p)}, u^{(p)}, t^{(p)}) dt, \forall \theta \in \{1, \dots, n_{ens}\} \tag{5}$$

where each ensemble is denoted with θ, n_{ens} denotes the total number of ensembles and α_{θ} is the weight factor for each sampled trajectory, which is obtained by calculating the quadrature/cubature weights.
In this case, the optimization variables for the multi-phase optimization problem is:

$$z = \begin{bmatrix} z^{(1)} \\ \vdots \\ z^{(P)} \end{bmatrix} \tag{6}$$

DOI: 10.13009/EUCASS2023-396

where the variables for each phase, $z^{(p)}$ are defined as follows,

$$z^{(p)} = \begin{bmatrix} \chi_1^{(p)} \\ \vdots \\ \chi_{n_{ens}}^{(p)} \\ U^{(p)}{}_{:,1} \\ \vdots \\ U^{(p)}{}_{:,n_u^{(p)}} \\ \mathbb{U}_1^{(p)} \\ \vdots \\ \mathbb{U}_{n_{ens}}^{(p)} \\ \mathbb{T}_1^{(p)} \\ \vdots \\ \mathbb{T}_{n_{ens}}^{(p)} \end{bmatrix} \tag{7}$$

$$\chi_{\theta_{(p)}}^{(p)} = \begin{bmatrix} Y_{\theta\ :,1}^{(p)} \\ \vdots \\ Y_{\theta_{(p)}:,n_y^{(p)}}^{(p)} \end{bmatrix}, \forall\theta_{(p)} \in \left\{1,\ldots,n_{ens}{}^{(p)}\right\} \tag{8}$$

$$\mathbb{U}_{\theta_{(p)}}^{(p)} = \begin{bmatrix} U_{rec,\theta_{(p)}:,1}^{(p)} \\ \vdots \\ U_{rec,\theta_{(p)}:,n_u^{(p)}}^{(p)} \end{bmatrix}, \forall\theta_{(p)} \in \left\{1,\ldots,n_{ens}{}^{(p)}\right\} \tag{9}$$

$$\mathbb{T}_{\theta_{(p)}}^{(p)} = \begin{bmatrix} t_0{}_{\theta_{(p)}}^{(p)} \\ t_f{}_{\theta_{(p)}}^{(p)} \end{bmatrix}, \forall\theta_{(p)} \in \left\{1,\ldots,n_{ens}{}^{(p)}\right\} \tag{10}$$

$\chi_{\theta_{(p)}}^{(p)}$ is the state vector, $\mathbb{U}_{\theta_{(p)}}^{(p)}$ is the closed-loop (and recovery control when used together with the open-loop control) control input vector and $\mathbb{T}_{\theta_{(p)}}^{(p)}$ is the vector for the time variables for the sample $\theta_{(p)}$ and phase p. On the other hand, $U^{(p)}{}_{:,n_u^{(p)}}$ is the nominal control for all the ensembles and used as open-loop control input. Time vector is defined as $\mathbb{T}_{(p)} \in \mathbb{R}^{2n_{ens}{}^{(p)}x1}$ for closed-loop guidance phase and $\mathbb{T}_{(p)} \in \mathbb{R}^{2x1}$ for open-loop guidance phase. Lastly, the endpoint vector is defined as:

$$e_\theta{}^{(P)} = \left[Y_{\theta\ \ 1,:}^{(p)}, t_0{}_{\theta_{(p)}}^{(p)}, Y_{\theta\ \ (N+1)^{(p)},:}^{(p)}, t_f{}_{\theta_{(p)}}^{(p)}\right], \quad \forall p \in \{1,\ldots,P\} \tag{11}$$

as a result, resulting optimization variable of each phase is:

$$z^{(P)} \in \mathbb{R}^{\left[(N^{(p)}+1)\times n_y^{(p)}\times n_{ens}{}^{(p)}+N^{(p)}n_u^{(p)}\times(n_{ens}{}^{(p)}+1)+2n_{ens}{}^{(p)}\right]x1} \tag{12}$$

Dynamic and path constraints are calculated as,

$$A_\theta{}^{(p)} = \begin{bmatrix} a^{(p)}\left(Y_{\theta 1,:}{}^{(p)}, U_{1,:}{}^{(p)}, U_{rec,\theta_{(p)}1,:}^{(p)}, \mathbb{T}_{\theta_{(p)}}^{(p)}\right) \\ \vdots \\ a^{(p)}(Y_{\theta N^{(p)},:}{}^{(p)}, U_{N^{(p)},:}{}^{(p)}, U_{rec,\theta_{(p)}N,:}^{(p)}, \mathbb{T}_{\theta_{(p)}}^{(p)}) \end{bmatrix} \in \mathbb{R}^{N^{(p)}x\ n_y^{(p)}}$$

$$C_\theta{}^{(p)} = \begin{bmatrix} c^{(p)}\left(Y_{\theta 1,:}{}^{(p)}, U_{1,:}{}^{(p)}, U_{rec,\theta_{(p)}1,:}^{(p)}, \mathbb{T}_{\theta_{(p)}}^{(p)}\right) \\ \vdots \\ c^{(p)}(Y_{\theta N^{(p)},:}{}^{(p)}, U_{N^{(p)},:}{}^{(p)}, U_{rec,\theta_{(p)}N,:}^{(p)}, \mathbb{T}_{\theta_{(p)}}^{(p)}) \end{bmatrix} \in \mathbb{R}^{N^{(p)}x\ n_y^{(p)}} \tag{13}$$

and $A^{(p)}$ and $C^{(p)}$ are formed simply by concatenation of these matrices in third dimension.

DOI: 10.13009/EUCASS2023-396

As a result, the ensemble optimal control problem is rewritten in terms of the following constraints:

$$\left(\triangle^{\theta}{}_{i}\right)^{(p)} = \frac{dy_i^{\theta}(t)}{dt} - \frac{t_f{}^{(p)} - t_0{}^{(p)}}{2} A_{\theta}^{(p)} = D^{(p)} Y_i^{\theta} - \frac{t_f{}^{(p)} - t_0{}^{(p)}}{2} A_{\theta}^{(p)} = 0, \ \forall i \in \left\{1, \ldots, N_k^{(p)}\right\} \tag{14}$$

$$c^{(p)}{}_{min} \le C_{i,:}^{(\theta,p)} \le c^{(p)}{}_{max}, \qquad \forall p \in \{1, \ldots, P\} \qquad \forall i \in \{1, \ldots, N^p\} \tag{15}$$

$$b_{min} \le b(e_{\theta}^{(1)}, \ldots, e_{\theta}^{(p)}) \le b_{max} \tag{16}$$

$\left(\triangle^{\theta}{}_{i}\right)^{(p)}$ are the dynamic deficit constraints, $N^{(p)} = \sum_{k=1}^{K(p)} N_k^{(p)}$ is the total number of quadrature nodes for the corresponding phase, $w^{(p)} \in \mathbb{R}^{N(p)}$ is the vector consisting of quadrature weights and $D^{(p)}$ is the pseudospectral differentiation matrix.

2.2 Recovery Ensemble Control

Recovery ensemble control aims to generate safe, optimal and adaptive trajectory reshaping strategies. Contrary to desensitized optimal control and integrated guidance and control optimization frameworks, the proposed strategy controls the ensemble of uncertainty space to satisfy the hard constraints by minimizing the so-called recovery control without imposing any structure, for example linear feedback control, and optimizes a nominal control for all the ensembles. These recovery controls are a function of dispersed states and the uncertain variables, therefore they can be used for generating a database of feedback control policies for different combinations of uncertainties. Rather than minimizing the deviation from a predetermined robust and safe reference trajectory, REC minimizes the deviation from their respective true optimal trajectory with a tradeoff variable called as recovery weight (ω_{rec}). In this research, Time-dependent Recovery Ensemble Control (T-REC) is utilized for the boost-back and re-entry phases of reusable launch vehicles.
Objective function for the optimal control problems using this concept can be formulated as follows:

$$J = \mathbb{E}\left[-m\left(t_f\right) + \frac{\omega_{rec}}{2} \int_{t_0}^{t_f} \left|u_{recovery}\right|^2 dt\right] \tag{17}$$

which can be approximated via cubature-rule based approaches as follows:

$$J = \sum_{\theta} \alpha_{\theta} \left[-m^{\theta}\left(t_f\right) + \frac{\omega_{rec}}{2} \int_{t_0}^{t_f} \left|u_{recovery,\theta}\right|^2 dt\right] \tag{18}$$

where θ denotes the ensembles, which refers to different possible system parameters, α_{θ} is the cubature weight and ω_{rec} is a weighting parameter that represents the importance of the recovery control terms in the objective function. In the case of $\omega_{rec} = 0$, optimal results correspond to finding deterministic optimal controls for each of the ensembles. In the second extreme case, as $\omega_{rec} \to \infty$, the optimal solution becomes the robust open-loop control input, which is an ensemble optimal control solution in which the same control input is applied to all ensembles. However, resulting problem may become infeasible due to the final boundary constraints. By tuning the aforementioned recovery weight, resulting optimized open-loop control input is said to be partially-robust, resulting in different magnitudes of corrective controls. In this case, total control for each ensemble is defined as follows:

$$u_{\alpha} = u_{nominal} + u_{recovery,\alpha} \tag{19}$$

In the previous research on REC,[43] it was shown that costate dynamics of the system depends on both the nominal control and the recovery control for the corresponding ensemble and are independent from each other. On the other hand, the nominal control depends on all of the ensemble costates, and recovery control terms can be derived from the costates and the nominal control. This means that the nominal control can be used to derive recovery control terms that compensate for uncertainties in the system parameters.

3. Test Cases

Benchmark problems are taken from the references.[36,37] A systematic comparison has been conducted between different hybrid guidance architectures with robust optimization and REC. Numerous comparisons studied in this research are summarized in Fig. 1. We systematically compare the results for two scenarios under I_{sp}, thrust, atmospheric density and axial aerodynamic uncertainties.

DOI: 10.13009/EUCASS2023-396

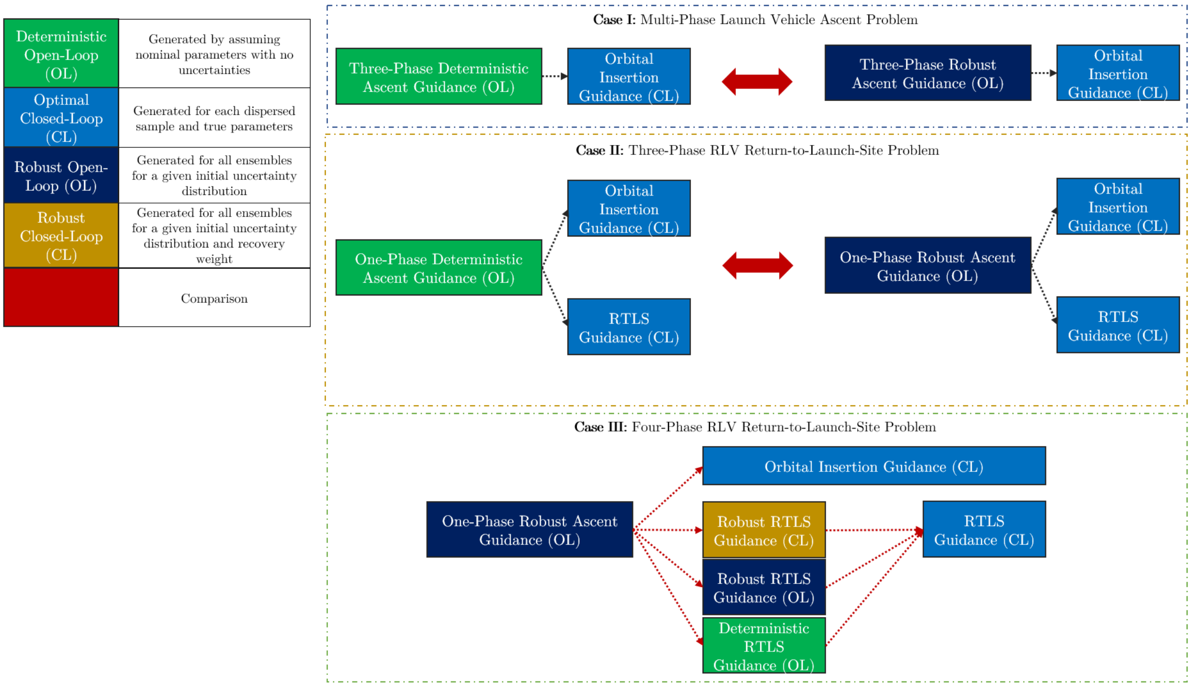

Figure 1: Systematic Comparison and Robust Optimization of Different Hybrid Guidance Architectures

In both of the problems, the optimal control problem is transformed into a Mayer problem as follows:

$$J = -m^{(4)}(t_{f,4}) \tag{20}$$

Governing equations for the motion of the launch vehicle are given as follows:

$$\dot{\vec{r}} = \vec{v} \tag{21}$$

$$\dot{\vec{v}} = -\frac{\mu}{\left|\vec{r}\right|^3}\vec{r} + \frac{\vec{T}}{m} + \frac{\vec{D}}{m} \tag{22}$$

$$\dot{m} = -\frac{\left|\vec{T}\right|}{g_0 I_{sp}} \tag{23}$$

$$\tag{24}$$

where,

$$\vec{D} = -\frac{1}{2}\rho_0 e^{-\frac{h}{H}} S\, C_D \left|\vec{v}_{rel}\right| \vec{v}_{rel} \tag{25}$$

$$\vec{v}_{rel} = \vec{v} - [0\; 0\; \Omega_E]^T \times \vec{r} \tag{26}$$

and $G = g_0 \left(\frac{R_e}{R_e + r}\right)^2$, subjected to the following path constraints:

$$\frac{1}{2}\rho \left|\vec{v}_{rel}\right|^2 \leq q_{max} \tag{27}$$

in which the 80 kPa maximum dynamic pressure is used for the second problem. In the given equations, R_e denotes the radius of Earth, ρ is the atmospheric density, S is the cross-sectional area, C_D is the drag coefficient of the stage, m is the mass, g_0 is the acceleration due to gravity in sea level and D is the drag force acting on the vehicle. $\vec{r}$ and $\vec{v}$ are the position and velocity vectors in ECI frame.

DOI: 10.13009/EUCASS2023-396

3.1 Ascent Trajectory Optimization

In the first case, an optimal control problem for a multi-phase launch vehicle ascent mission for Delta III rocket is studied to maximize the payload mass inserted into a GTO orbit with orbital elements:

$$a, e, i, \Omega, \omega = [24361.14\ km, 0.7308, 28.5°, 269.8°,\ 130.5°] \tag{28}$$

The mass, thrust and aerodynamic data are taken from the reference.[36]
In this study, a reference trajectory under nominal conditions is optimized and then based on the real trajectories that will be dispersed due to uncertainties, an expectation of the maximum payload that can be inserted into the orbit via closed-loop guidance algorithms is calculated. Then, an integrated optimization of both ascent and orbital insertion guidance is assessed with the use of SC-EPOCS to generate robust open-loop ascent trajectory and also the accompanying optimal guidance for orbital insertion for each dispersed state trajectory.

3.2 RTLS Trajectory Optimization

The reference article[37] solved two different scenarios, one is the RTLS and other is the Down-range Landing (DRL). In this subsection, the RTLS case is studied with a dynamic pressure constraint. The objective function is set to maximize the payload mass inserted into a target orbit, defined as:

$$a, e, i, \Omega, \omega = [6593.145\ km, 0.0076, 28.5°, 269.8°,\ 130.5°] \tag{29}$$

Major uncertainties including atmospheric density and aerodynamic uncertainties for reusable launch vehicles were studied in[44] and incorporated into the robust trajectory optimization framework together with thrust and specific impulse uncertainties.
Similar to the first scenario, deterministic optimal reference trajectory is optimized and then by obtaining the dispersed states under uncertainties, boostback, landing and orbital insertion trajectories are optimized assuming true parameters. Then the results are compared with the SC-EPOCS to evaluate the advantage of the robust open-loop ascent trajectory. Then, a more realistic scenario is studied by also including the uncertainties in boostback till the landing maneuver. In this case the original problem is cast as a four-phase optimal control problem where the last phase is initiated at most 200 seconds before the landing maneuver. To assess the impact of including closed-loop corrections to the boostback maneuver, we generate optimal and robust control laws via recovery ensemble control for different recovery weights to study the tradeoff between robustness and propellant margins and compare it with the open-loop robust boostback maneuver.
Note that the robust optimization results for the hybrid guidance architectures for the RTLS scenario only optimizes the worst-case landing guidance, since only the feasibility of the worst-case scenario impacts the optimization objective function, which is the final mass of the second stage.

4. Numerical Results

All of the simulations are performed with Matlab 2021b with AMD Ryzen 5 3500X processor, 16 GB of RAM and Nvidia GeForce RTX 2060 graphics card. IPOPT is used to solve the resulting the nonlinear programming problem with MA-45 linear solver. Absolute and relative convergence tolerance criterion was set to 10^{-10}. A Legendre-Gauss-Radau (LGR) mesh with 80 nodes for each phase was selected for the transcription of the optimization problems.
The uncertainties were modeled as uniform distributions for uncertain parameters and sampled with respect to the cubature rule generated by 4th order Conjugate Unscented Transformation.[42] $\pm 20\%$ uncertainty was assigned for the drag coefficient for both stages (c_D), $\pm 5\%$ uncertainty was assigned for atmospheric density (ρ), and $\pm 1\%$ uncertainty was assigned for uncertainties in thrust and specific impulse of both stages. Finally, various recovery weights ω_{rec}, ranging between 10^{-3} and 10, were applied to evaluate their impact on the payload mass. In the following figures, the darker hues represent lower recovery weights.

4.1 Multi-phase Ascent Problem

Results shown in the Fig. 2 and 3 suggests that, contrary to the studies employed[22,23] where an open-loop guidance was designed to reduce the state dispersion at the end of orbital insertion and a tradeoff between optimality and dispersion was observed, in our study, robust optimization of open-loop phase has a very negligible performance improvement rather than reduction, about 1.25761 g. This is mainly a result of including closed-loop guidance in the optimization framework which can update the target insertion point for the exo-atmospheric flight.

DOI: 10.13009/EUCASS2023-396

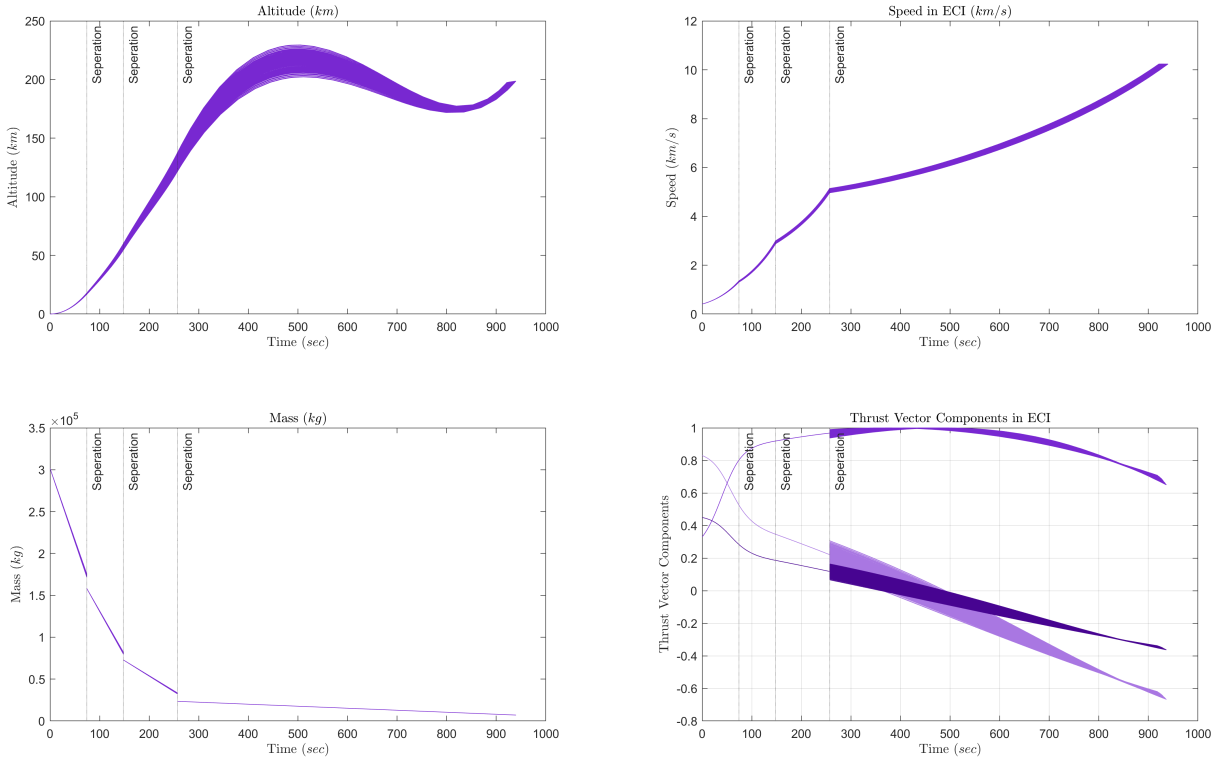

Figure 2: Optimized Multi-phase Ascent Launch Vehicle Trajectory and Control Inputs

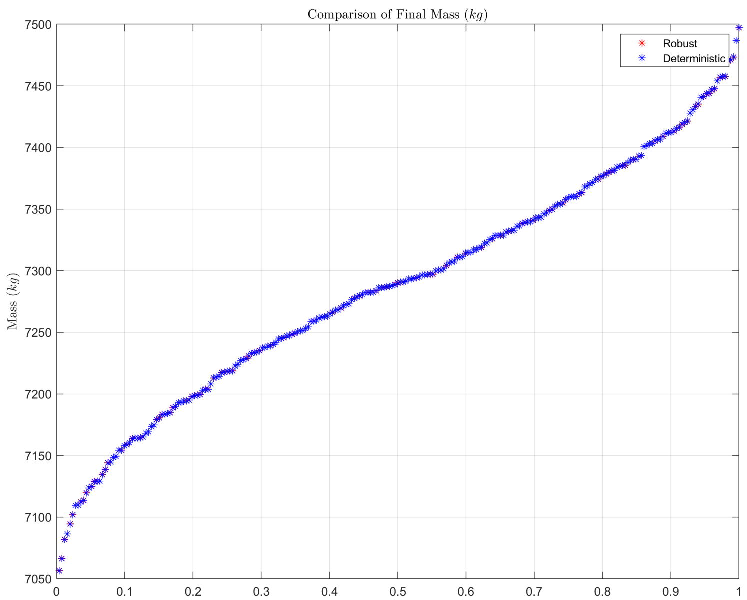

Figure 3: Comparison of Final Mass of the Launch Vehicle for Robust and Deterministic Open-loop Guidance

DOI: 10.13009/EUCASS2023-396

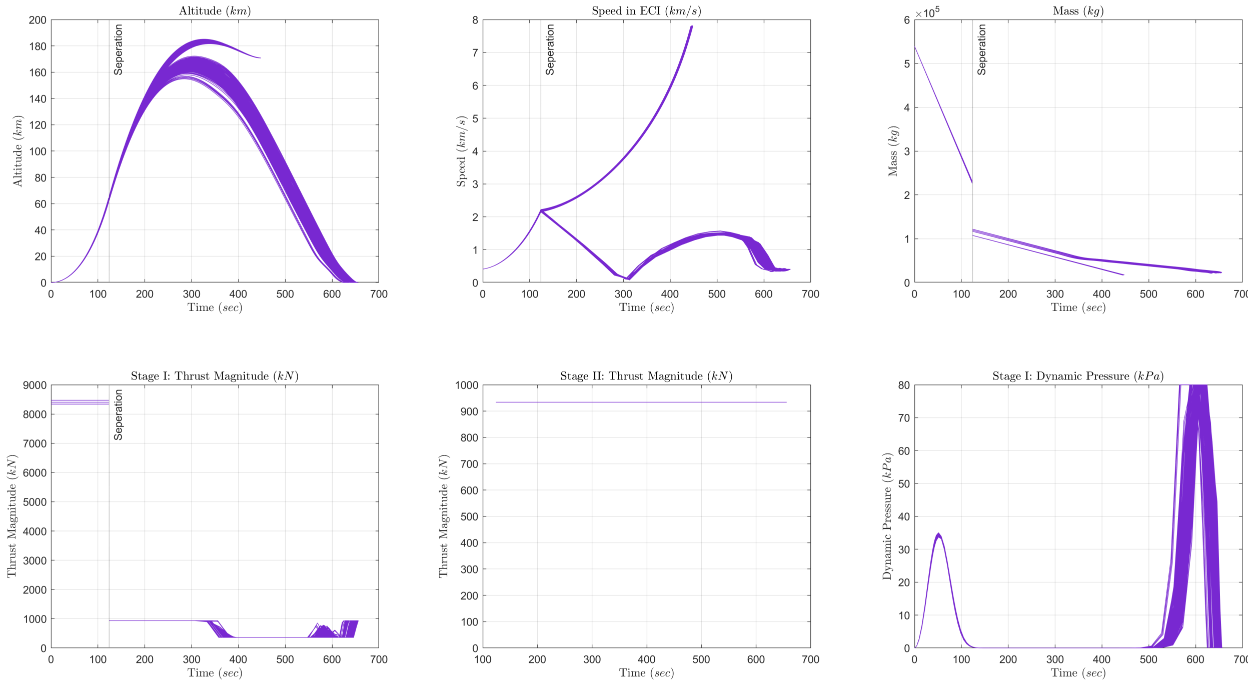

Figure 4: Optimized Deterministic Multi-phase RTLS Trajectory and Control Inputs under Uncertainties

4.2 Three-Phase RTLS Comparison

Results shown in the Fig. 4, 5 and 6 demonstrates the importance and advantage of integrated robust optimization of both open and closed-loop guidance. In Fig. 4, a deterministic open-loop guidance was used for the ascent phase. Although the mean of the final mass higher than robust open-loop guidance with 316.56022 kg, as a result of uncertainties, the launch vehicle couldn't achieve landing for almost half the cases as shown in Fig. 6, where in Fig. 5, the worst-case can achieve landing by utilizing all the propellant. This is similar to what would be expected for the deterministic optimal control problem, in which there is no unused propellant mass left for the first stage.

4.3 Four-Phase RTLS Comparison

Results shown in the following figures conclude the advantage of robust boostback and re-entry guidance and also the robust open-loop ascent guidance when compared to the previously studied deterministic open-loop ascent guidance. In Fig. 7, a robust open-loop ascent guidance and deterministic open-loop guidance for boostback and re-entry was used for landing. Similar to the previous study, the results shown in Fig. 10 demonstrates that the worst-case still can achieve landing by utilizing all the propellant. Also in the results shown in Fig. 9, sacrifice in the final mass of the second phase is about 11.34438 kg for different recovery weights while the advantage of including recovery ensemble control for the final mass of the first stage is 166.35875 kg. As can be expected, as the recovery weight increase, the results converged towards the robust optimization results, indicated in Fig. 8. It is important to note that, due to the robust open-loop ascent guidance, the dispersions were quite low compared to open-loop ascent guidance studied in the previous case and therefore, even when the vehicle generates a open-loop guidance for boostback and re-entry, in almost each case the landing can be successfully performed with the available propellant.

5. Conclusion

In this research, a new computational framework is developed to systematically optimize both robust open-loop and closed-loop guidance modes to study their advantages, yielding a hybrid guidance architecture that mitigates the impact of uncertainties in aerodynamic density, axial aerodynamic forces, thrust and specific impulse of the engines and also generate realistic design margins. Two benchmark multi-phase launch vehicle optimization problems were studied, one is the Delta-III ascent mission and second is the RTLS mission for reusable launch vehicles. In-house developed SC-EPOCS is used to solve the resulting multi-phase ensemble control problems together with recovery ensemble control and CUT. Results suggested that while there was no apparent advantage of robust optimized hybrid guidance

DOI: 10.13009/EUCASS2023-396

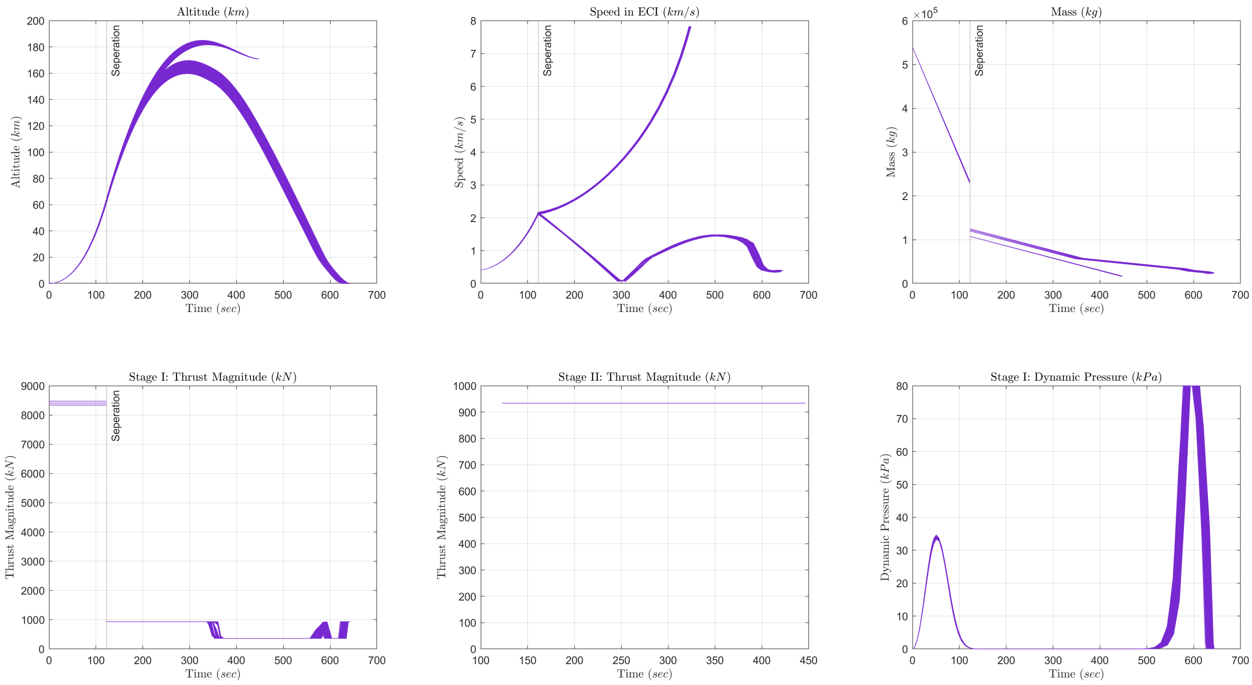

Figure 5: Optimized Robust Multi-phase RTLS Trajectory and Control Inputs under Uncertainties

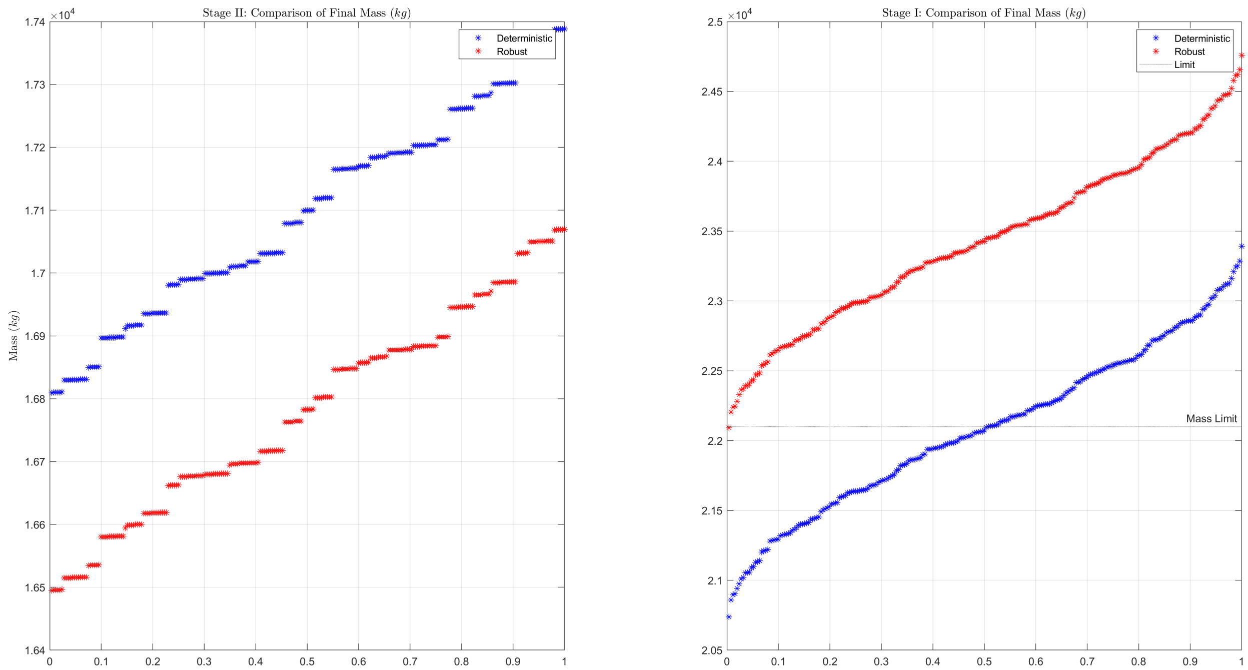

Figure 6: Comparison of Final Masses of First and Second Stage of the Launch Vehicle for Robust and Deterministic Open-loop Ascent Guidance

DOI: 10.13009/EUCASS2023-396

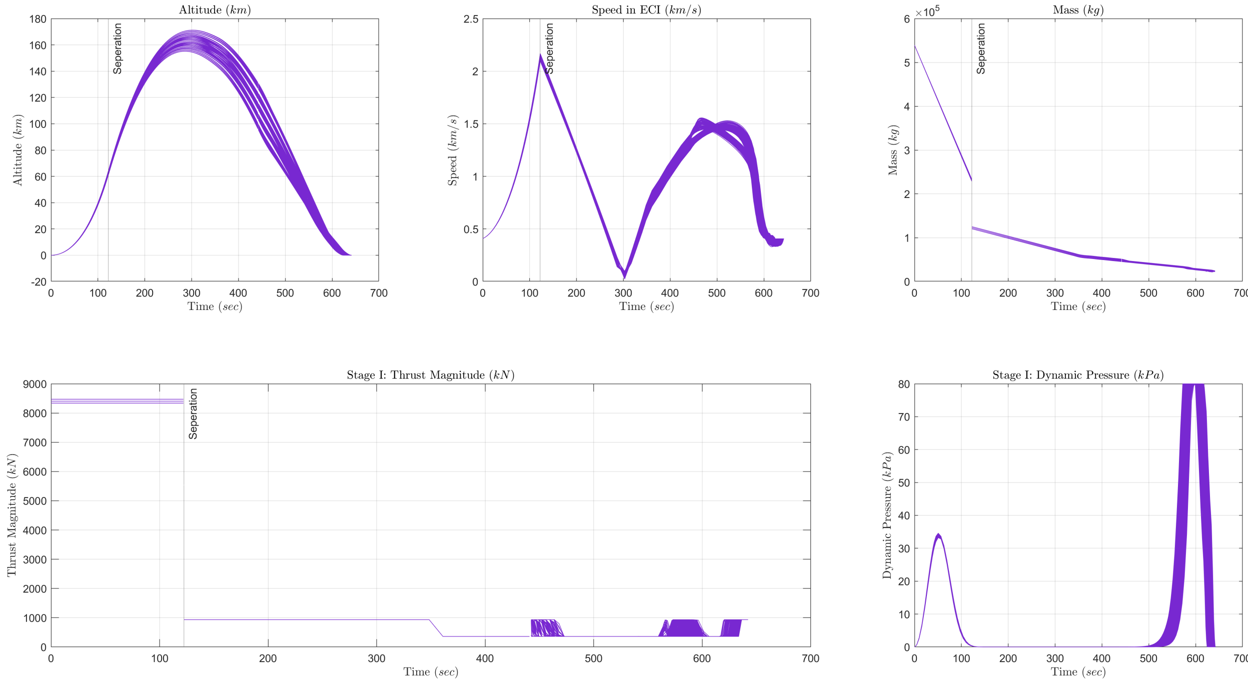

Figure 7: Optimized Deterministic Multi-phase RTLS Trajectory and Control Inputs with Robust Open-loop Ascent Guidance under Uncertainties

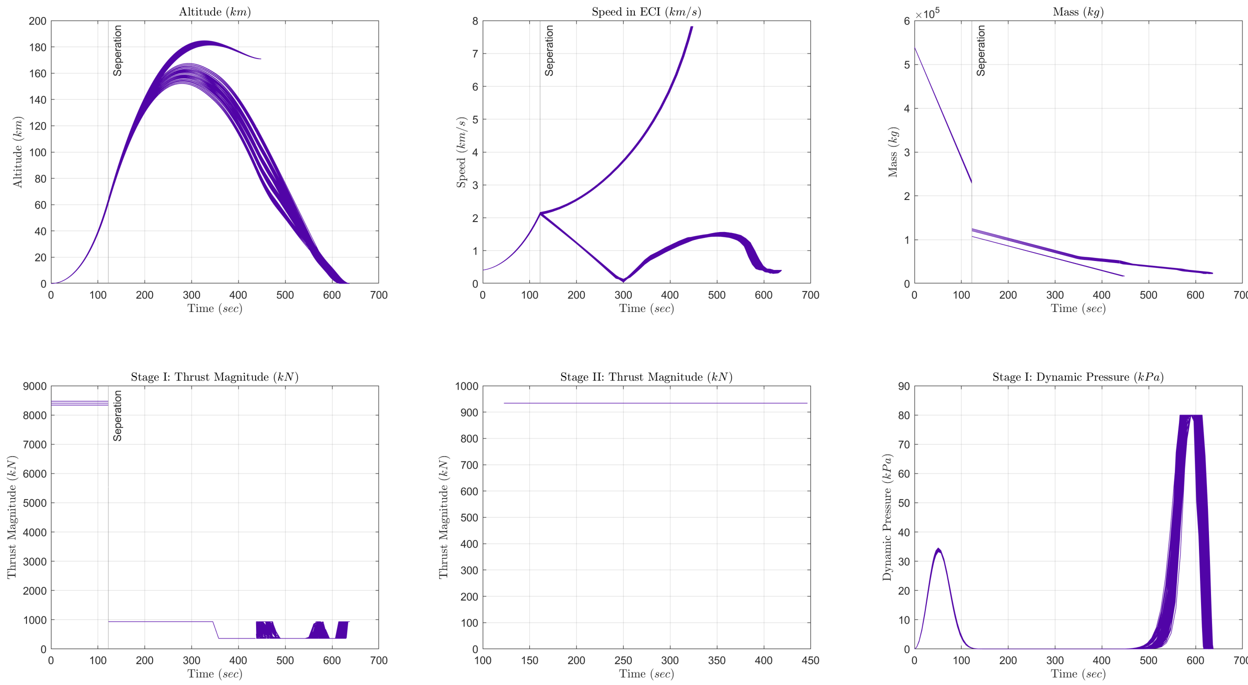

Figure 8: Optimized Robust Multi-phase RTLS Trajectory and Control Inputs under Uncertainties

DOI: 10.13009/EUCASS2023-396

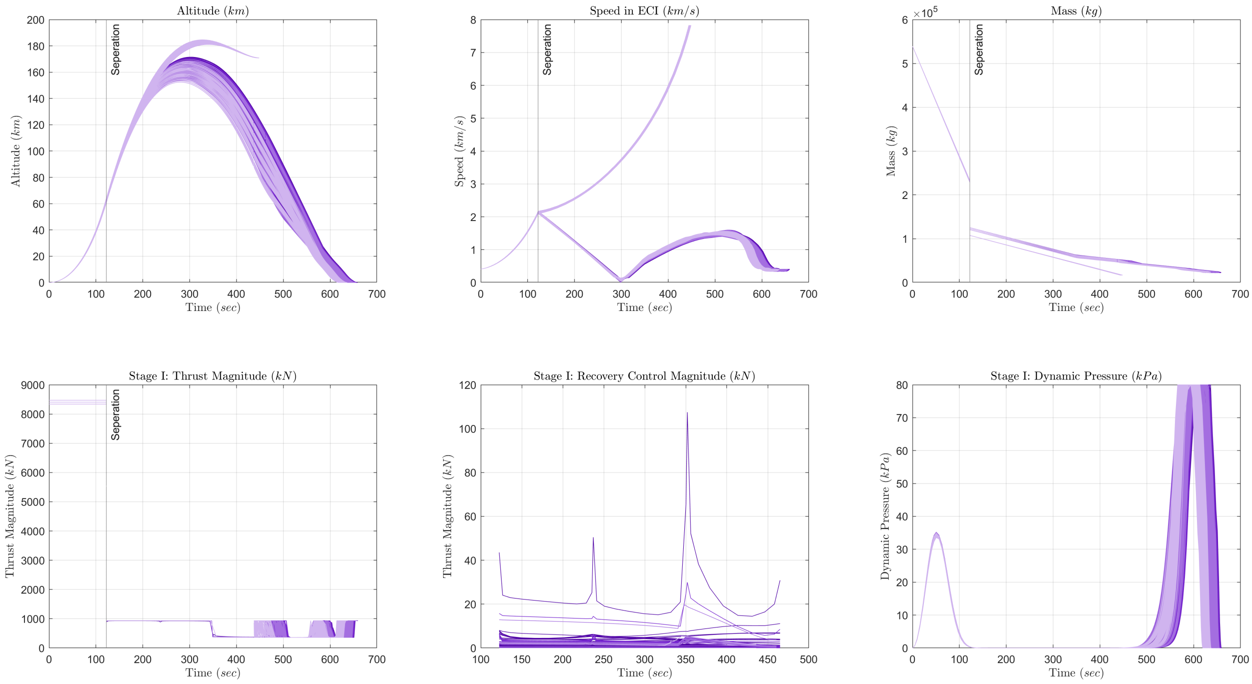

Figure 9: Optimized Partially-Robust Multi-phase RTLS Trajectory and Control Inputs under Uncertainties (Darker tones indicate lower recovery weights)

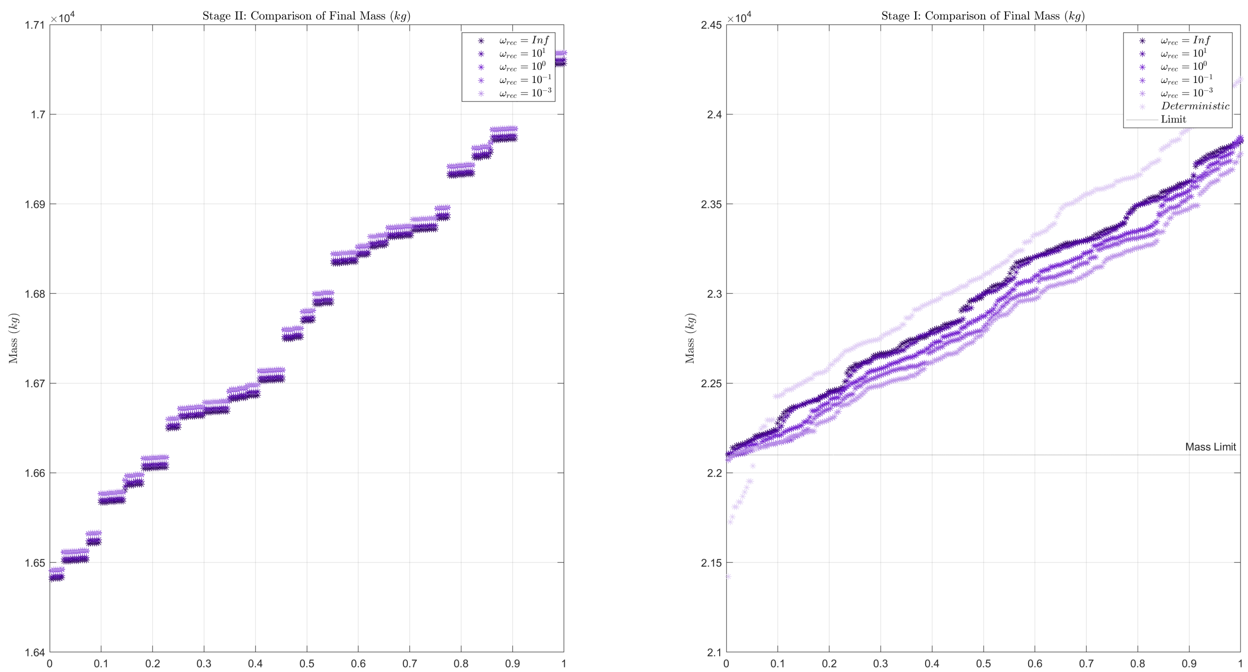

Figure 10: Comparison of Final Masses of First and Second Stage of the Launch Vehicle for Robust and Deterministic Open-loop Ascent, Boostback and Re-entry Guidance

DOI: 10.13009/EUCASS2023-396

for the ascent mission, it is concluded that complex missions such as RTLS has great benefits in terms of systematically assigning design margins for the required propellant and also safe reference trajectories and reshaping strategies.

References

[1] Boris Benedikter, Alessandro Zavoli, Zhenbo Wang, Simone Pizzurro, and Enrico Cavallini. *Covariance Control for Stochastic Low-Thrust Trajectory Optimization*. 2022.

[2] Jack Ridderhof and Panagiotis Tsiotras. *Uncertainty Quantication and Control During Mars Powered Descent and Landing using Covariance Steering*. 2018.

[3] Nicola Marmo, Alessandro Zavoli, Naoya Ozaki, and Yasuhiro Kawakatsu. A hybrid multiple-shooting approach for covariance control of interplanetary missions with navigation errors. In *33rd AAS/AIAA Space Flight Mechanics Meeting*, 01 2023.

[4] Kenshiro Oguri, Gregory Lantoine, and Theodore H. Sweetser. *Robust Solar Sail Trajectory Design under Uncertainty with Application to NEA Scout Mission*. 2022.

[5] Kenshiro Oguri and Gregory Lantoine. Stochastic sequential convex programming for robust low-thrust trajectory design under uncertainty. In *AAS/AIAA Astrodynamics Specialist Conference*, 08 2022.

[6] Boris Benedikter, Alessandro Zavoli, Guido Colasurdo, Simone Pizzurro, and Enrico Cavallini. Stochastic control of launch vehicle upper stage with minimum-variance splash-down. 09 2022.

[7] Ming Xu, Tian Tan, and Shijie Xu. Stochastic optimal maneuver strategies for transfer trajectories. *Journal of Aerospace Engineering*, 27(2):225–237, 2014.

[8] Remy Derollez, Simon Le Cleac'h, and Zachary Manchester. Robust entry vehicle guidance with sampling-based invariant funnels. In *2021 IEEE Aerospace Conference (50100)*, pages 1–9, 2021.

[9] Naoya Ozaki, Stefano Campagnola, and Ryu Funase. Tube stochastic optimal control for nonlinear constrained trajectory optimization problems. *Journal of Guidance, Control, and Dynamics*, 43(4):645–655, 2020.

[10] Naoya Ozaki and Ryu Funase. *Tube Stochastic Differential Dynamic Programming for Robust Low-Thrust Trajectory Optimization Problems*.

[11] David Woffinden, Simon Shuster, David Geller, and Stefan Bieniawski. Robust trajectory optimization and gnc performance analysis for nrho rendezvous. In *AAS/AIAA Astrodynamics Specialist Conference*, 08 2022.

[12] Masahiro Fujiwara and Ryu Funase. Observability-aware and robust trajectory optimization for small-body gravity estimation. In *31st AAS/AIAA Space Flight Mechanics Meeting*, 02 2021.

[13] Kenshiro Oguri and Jay W. McMahon. Robust spacecraft guidance around small bodies under uncertainty: Stochastic optimal control approach. *Journal of Guidance, Control, and Dynamics*, 44(7):1295–1313, 2021.

[14] Kenshiro Oguri and Jay Mcmahon. Risk-aware trajectory design with continuous thrust: Primer vector theory approach. 08 2019.

[15] Kenshiro Oguri and Jay Mcmahon. Risk-aware trajectory design with impulsive maneuvers: Convex optimization approach. 08 2019.

[16] Cristian Greco, Stefano Campagnola, and Massimiliano L. Vasile. *Robust Space Trajectory Design using Belief Stochastic Optimal Control*.

[17] Yuechen Huang, Haiyang Li, Xin Du, and Xiangyue He. Mars entry trajectory robust optimization based on evidence under epistemic uncertainty. *Acta Astronautica*, 163:225–237, 2019. Fourth IAA Conference on Dynamics and Control of Space Systems (DYCOSS2018).

[18] J Roshanian, AA Bataleblu, and M Ebrahimi. A novel metamodel management strategy for robust trajectory design of an expendable launch vehicle. *Proceedings of the Institution of Mechanical Engineers, Part G: Journal of Aerospace Engineering*, 234(2):236–253, 2020.

[19] Loic Brevault and Mathieu Balesdent. Uncertainty quantification for multidisciplinary launch vehicle design using model order reduction and spectral methods. *Acta Astronautica*, 187:295–314, 2021.

DOI: 10.13009/EUCASS2023-396

[20] Anirban Chaudhuri, Garrett Waycaster, Nathaniel Price, Taiki Matsumura, and Raphael T. Haftka. Nasa uncertainty quantification challenge: An optimization-based methodology and validation. *Journal of Aerospace Information Systems*, 12(1):10–34, 2015.

[21] Yuechen Huang, Haiyang Li, Xin Du, and Xiangyue He. Mars entry trajectory robust optimization based on evidence under epistemic uncertainty. *Acta Astronautica*, 163:225–237, 2019. Fourth IAA Conference on Dynamics and Control of Space Systems (DYCOSS2018).

[22] Reza Zardashti, Mahdi Jafari, Sayyed Hosseini, and Seyyed Ali Saadatdar Arani. Robust optimum trajectory design of a satellite launch vehicle in the presence of uncertainties. *Journal of Aerospace Technology and Management*, 12, 08 2020.

[23] Jafar Roshanian, Ali A Bataleblu, and Masoud Ebrahimi. Robust ascent trajectory design and optimization of a typical launch vehicle. *Proceedings of the Institution of Mechanical Engineers, Part C: Journal of Mechanical Engineering Science*, 232(24):4601–4614, 2018.

[24] Fenfen Xiong, Ying Xiong, and Bin Xue. *Trajectory Optimization under Uncertainty based on Polynomial Chaos Expansion*.

[25] Reliability-based trajectory optimization using nonintrusive polynomial chaos for mars entry mission. *Advances in Space Research*, 61(11):2854–2869, 2018.

[26] Xiang Li, Prasanth B. Nair, ZhiGang Zhang, Lin Gao, and Chen Gao. Aircraft robust trajectory optimization using nonintrusive polynomial chaos. *Journal of Aircraft*, 51(5):1592–1603, 2014.

[27] James Fisher and Raktim Bhattacharya. Optimal trajectory generation with probabilistic system uncertainty using polynomial chaos. *Journal of Dynamic Systems, Measurement, and Control*, 133:014501, 01 2011.

[28] Fenggang Wang, Shuxing Yang, FenFen Xiong, Qizhang Lin, and Jianmei Song. Robust trajectory optimization using polynomial chaos and convex optimization. *Aerospace Science and Technology*, 92:314–325, 2019.

[29] Doris C. Chandler and Isaac E. Smith. Development of the iterative guidance mode with its application to various vehicles and missions. *Journal of Spacecraft and Rockets*, 4(7):898–903, 1967.

[30] R. Jaggers. *An explicit solution to the exoatmospheric powered flight guidance and trajectory optimization problem for rocket propelled vehicles*.

[31] Boris Benedikter, Alessandro Zavoli, Guido Colasurdo, Simone Pizzurro, and Enrico Cavallini. Convex approach to three-dimensional launch vehicle ascent trajectory optimization. *Journal of Guidance, Control, and Dynamics*, 44:1–16, 04 2021.

[32] Marco Sagliano, David Seelbinder, and Stephan Theil. *Autonomous Descent Guidance via Sequential Pseudospectral Convex Programming*. 04 2023.

[33] Yue Yu, Purnanand Elango, Behcet Acikmese, and Ufuk Topcu. Extrapolated proportional-integral projected gradient method for conic optimization. *IEEE Control Systems Letters*, 7:73–78, 2023.

[34] Abhinav G. Kamath, Purnanand Elango, Taewan Kim, Skye Mceowen, Yue Yu, John M. Carson, Mehran Mesbahi, and Behcet Acikmese. *Customized Real-Time First-Order Methods for Onboard Dual Quaternion-based 6-DoF Powered-Descent Guidance*.

[35] Pedro Simplicio, Andres Marcos, and Samir Bennani. Guidance of reusable launchers: Improving descent and landing performance. *Journal of Guidance, Control, and Dynamics*, pages 1–14, 08 2019.

[36] John Betts. Practical methods for optimal control and estimation using nonlinear programming. 19, 01 2010.

[37] Lin Ma, Kexin Wang, Zhijiang Shao, Zhengyu Song, and Lorenz Biegler. Direct trajectory optimization framework for vertical takeoff and vertical landing reusable rockets: case study of two-stage rockets. *Engineering Optimization*, 51:1–19, 07 2018.

[38] Akan Selim and Ibrahim Ozkol. Development and validation of a modular and multi-phase pseudospectral optimal control software (in turkish). In *8. Ulusal Havacilik ve Uzay Konferansi*, 09 2022.

DOI: 10.13009/EUCASS2023-396

[39] Akan Selim. Robust trajectory optimization of constrained re-entry flight via stochastic collocation based ensemble pseudospectral optimal control. Master's thesis, Istanbul Technical University, 09 2022.

[40] Akan Selim and Ibrahim Ozkol. Real-time optimal control of a 6-dof state-constrained close-proximity rendezvous mission. *Acta Astronautica*, 211:280–294, 2023.

[41] Akan Selim and Ibrahim Ozkol. Robust trajectory optimization of constrained re-entry flight. In *10th International Conference on Recent Advances in Air and Space Technologies (RAST 2023)*, 06 2023.

[42] Nagavenkat Adurthi, Puneet Singla, and Tarunraj Singh. The conjugate unscented transform an approach to evaluate multi-dimensional expectation integrals. In *2012 American Control Conference (ACC)*, pages 5556–5561, 2012.

[43] Akan Selim and Ibrahim Ozkol. Safe and adaptive trajectory reshaping of constrained re-entry flight: Recovery ensemble control. In *25th AIAA International Space Planes and Hypersonic Systems and Technologies Conference*, 06 2023.

[44] Jian Zhao, Haiyang Li, Xiangyue He, Huang Yuechen, and Jianghui Liu. Uncertainty analysis for return trajectory of vertical takeoff and vertical landing reusable launch vehicle. *Mathematical Problems in Engineering*, 2020:1–18, 07 2020.